3.5 SCCMS projects

Developments of Machine Learning Solvers

Yusuke Nomura, Andrew S. Darmawan, Youhei Yamaji, Masatoshi Imada

Department of Applied Physics

The University of Tokyo, Hongo 7-3-1, Bunkyo-ku, Tokyo 113-8656

Developing accurate solvers to analyze strongly-correlated systems is a great challenge in condensed-matter physics. Recently, a new form of variational wave function written in terms of restricted Boltzmann machines (RBM) has been proposed [1]. In the RBM wave function, on top of physical spin degrees of freedom (visible spins in the visible layer), we introduce additional degrees of freedom (neurons in the hidden layer). The variational parameters are magnetic fields (bias terms) on visible and hidden spins and the coupling between visible and hidden layers. Then, the quantum correlations among physical variables are taken into account through the couplings to hidden neurons. The RBM wave functions have been shown to give better accuracy for transverse-field Ising and Heisenberg models than those of the tensor-network wave functions [1].

In this project, we have improved the accuracy and extend the range of application of the RBM-based machine learning solver. We have developed i) RBM solver combined with many-variable Monte Carlo (mVMC) method [2] and ii) an exact scheme to construct deep Boltzmann machines to represent ground states of many-body Hamiltonians [3].

In i), we have written down the variational wave function by combining concepts from machine leaning (RBM) and physics (pair-product (PP) wave function), which we call RBM+PP wave function. The RBM allows for flexible and unbiased representations of quantum states. The PP (geminal) wave function is used in the mVMC method [4] and describes nonlocal entanglement properly. The combined RBM+PP wave function can be applied not only to bosonic models but also to fermionic models. The RBM+PP substantially improves the accuracy beyond that ever achieved by RBM and mVMC method separately, thus proving its power as an accurate solver.

In ii) we have shown a deterministic approach to generate deep-Boltzmann-machine (DBM) network to represent ground states of many-body lattice Hamiltonians, using much more flexible representability of the DBM compared to the RBM [5]. The approach reproduces the exact imaginary-time Hamiltonian evolution by dynamically modifying the DBM parameters. The number of neurons grows linearly with the system size and

imaginary time, respectively. The physical quantities can be measured by the Monte Carlo sampling of both the visible and hidden variables for the constructed network. The present construction of classical DBM network provides a novel framework of quantum-to-classical mappings (in special cases, it becomes equivalent to the path integral formalism).

A part of this work has been done in collaboration with Giuseppe Carleo.

References

[1] G. Carleo and M. Troyer, Science **355**, 602 (2017).

[2] Y. Nomura, A. S. Darmawan, Y. Yamaji, and M. Imada Phys. Rev. B **96**, 205152 (2017).

[3] G. Carleo, Y. Nomura, and M. Imada, arXiv:1802.09558.

[4] D. Tahara and M. Imada, J. Phys. Soc. Jpn. 77, 114701 (2008).

[5] X. Gao and L.-M. Duan, Nature Communications **8**, 662 (2017).

First-Principles Phase Field Mapping

Kaoru Ohno

Department of Physics, Faculty of Engineering Science,

Yokohama National University, Tokiwadai, Hodogaya-ku, Yokohama 240-8501

Theoretical understanding of microstructure is very important in predicting the durability and performance of alloys. For this purpose, phase field models have been widely used to simulate the time evolution of microstructures and various properties. However, the results strongly depend on the input parameters, which are mostly empirical. Therefore, we propose a new and simple method to determine the input parameters purely from first principles. We calculate the free energy (Fig. 1) using cluster expansion method including atomic vacancies in combination with potential renormalization theory [1]. Then, the chemical potential is obtained as the free energy difference. The validity of the present method is tested for Ni-Al alloy systems. Our results clearly distinguish the local composition of alloys in accord with the experimental phase diagram (Fig 2). We have also succeeded in predicting the time evolution of microstructures of Ni-Al alloys at different compositions at 1300K (Fig. 3) [2].

References

[1] Y. Misumi, S. Masatsuji, R. Sahara, S. Ishii, and K. Ohno, J. Chem. Phys. **128**, 234702 (2008).

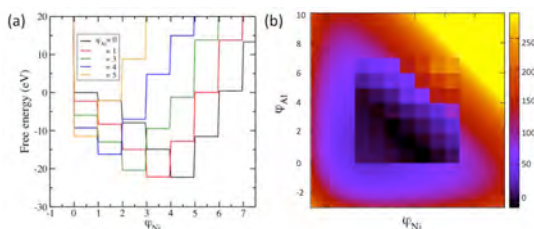[2] S. Bhattacharyya, R. Sahara and K. Ohno, to be submitted.
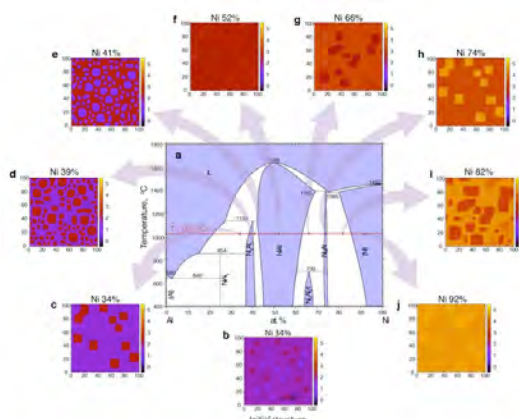
Fig. 1 Resulting free energy (a) 1D, (b) 2D.
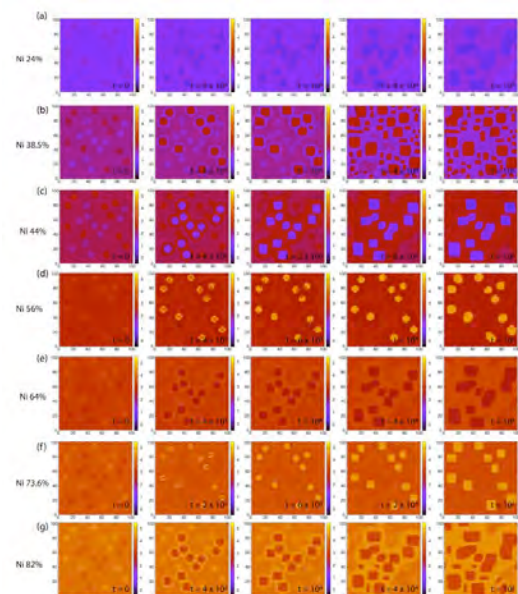

Fig. 2 Comparison with experimental PD.

Fig. 3 Time evolution of the pattern.

Oxide electrocatalyst

Osamu Sugino

Institute for Solid State Physics,

The University of Tokyo, Kashiwa-no-ha, Kashiwa, Chiba 277-8581

The purpose of this study is to predict the mechanism for oxygen reduction reaction (ORR) occurring on titania surfaces and to show a way to improve the ORR activity. For this purpose, we have done a first-principles simulation based on the density functional theory (DFT) within a generalized gradient approximation (GGA), which has been used as a standard method to simulate the titania surfaces. To model the surface, we are based on the experimental finding that doped Nb atom and the oxygen vacancy are the key to enhance the ORR activity. We have thus analyzed the surface of $Ti_xNb_yO_z$. In fact, we have simulated for rutile (110) and anatase (101),(100),(001),(001)-(1x4) surfaces with and without the surface Nb impurity and surface oxygen vacancy. Using those surfaces, we followed the ORR pathways by calculating the free-energy of O_2, OOH, OH, and O and obtained the free-energy profile. In the calculation, we have used the computational electrode scheme assuming zero for pH and 1.23 V vs SHE for the bias potential. Here we neglected the solvation effect. With the modeling, we have investigated whether ORR is likely to occur on those surfaces or not. We can expect that ORR is likely occur when the free-energy profile along the ORR pathways is flat within the energy scale of about 1.0 eV; this is the criterion that has been used for Pt surfaces. This criterion is expected to be valid also for titania.

After checking that the pristine titania surface does not provide the free-energy profile flat within 2.0 eV, we investigated the defective surfaces. We first investigated the surface doped with a Nb impurity atom. The calculated result indicates that the free-energy profile is uphill by 1.3 eV when OH* is reduced to form H_2O. That is, this surface is poisoned by OH and activity is not expected. We next investigated the surface with oxygen vacancy. In this case we also included Nb impurity in the surface model because the surface energy becomes too high because of the lack of charge neutrality. When Nb is located close to the vacancy site, the surface energy is high but the energy is lowered when Nb is located apart; the precise position does not affect the result in this case. From the calculation we found that O* is strongly adsorbed with the adsorption energy

larger than 2.0 eV for all the surfaces we have investigated. This is due to the existence of Ti^{3+} which donates an electron toward O* to stabilize this reaction intermediate. These results apparently suggest that all the defective surfaces do not remain as a candidate for the reactive surface.

However, this is not the case in fact because of the following reason. We have neglected that the surface oxygen vacancy accepts electrons from OH* stabilizing this species. With this consideration, we have included this adsorbate molecule in the modeling. When this is considered, the surface O* was found to be moderately adsorbed on the surface satisfying the above criterion for the active surface. The oxygen molecule, however, is not adsorbed on

rutile (110) nor on anatase (101) and (100). O_2 is too strongly adsorbed on anatase (001)-(1x4). Therefore, only anatase (001) remains as the candidate for the reactive surface. By calculating the free-energy profile, we confirmed that this surface satisfied the criterion. Therefore, we have concluded that only anatase (001) can be expected as the active surface. The rate-determining step is suggested to be the OH* reduction and the activation energy will be larger than 0.85 eV.

From these theoretical studies, we have suggested it is important to design a material to weaken the OH* adsorption.

Mesoscale simulation approach for slow dynamics study of complex and glassy liquids

Hayato SHIBA and Hailong PENG

Institute for Materials Research, Tohoku University

2-1-1 Katahira, Aoba-ku, Sendai 980-8577

For this year, we have numerically studied the slow dynamics of ionic liquid materials and underlying fundamental properties of glassy systems.

1. Study of mesophase transition upon annealing of imidazolium-based ionic liquid with long-alkyl chain

We have performed molecular dynamics simulations of a 1-dodecyl-3-methylimidazolium hexafluorophosphate ([C12mim][PF6]) ionic liquid using a united-atom model. It turned out that the ionic liquid exhibits a second step relaxation at temperatures below a crossover point, where the diffusion coefficient shows Arrhenius to non-Arrhenius transition. Annealing below this crossover temperature makes isotropic-to-mesophase transition, where the smectic A phase or crystal-like smectic B phase forms. From hundreds of nanoseconds to microseconds are required for completing these transitions. A normal diffusion process is found for anions along the layer-normal and -lateral directions in the SmA phase, but only in the lateral directions in the SmB phase. Our results suggests that studying such long-time dynamics opens the way to further understanding of ionic liquids, both on the basic properties of its phase behavior and glasss tarnsitions and on the potential applications utilizing their its nanostructure [1].

2. Cage-relative variables for 2D glassy dynamics

The Principal Investigator for this project and his coworkers have recently revealed that long-wavelength fluctuation exists in two-dimensional (2D) glassy systems, having the same origin as that given by the Mermin-Wagner theorem for 2D crystalline solids. For this year, we have discussed the slow glassy liquids under confinement, for better characterization of long-wavelength Mermin Wagner fluctuation by means of a molecular dynamics simulation of a lightly supercooled liquid. We employ the cage-relative mean-square displacement (MSD), defined on relative displacement to its cage, to quantitatively separate the long-wavelength fluctuation from the original MSD. For increasing system size the amplitude of acoustic long wavelength fluctuations not only increases but shifts to later times causing a crossover with structural relaxation of caging particles. The dynamic correlation grows as the structural relaxation becomes slower with decreasing temperature, uncovering an overestimation by the four-point correlation function due to the long-wavelength fluctuation. These findings motivate the usage of cage-relative MSD as a starting point for analysis of 2D glassy dynamics [2].

References

[1] H. Shiba, M. Kubo, and H.-L. Peng: Phys. Chem. Chem. Phys., in press (2018).

[2] H. Shiba, P. Keim, and T. Kawasaki: J. Phys: Cond. Matter **30** (2018) 094004.

Tensor Network Calculation of Frustrated Quantum Spin Systems[1]

Naoki KAWASHIMA

Institute for Solid State Physics, University of Tokyo
Kashiwa-no-ha, Kashiwa, Chiba 277-8581

The greatest obstacle in studying frustrated quantum system is the notorious negative sign problem. Due to this difficulty, researchers do not have much choice other than numerical diagonalization of small clusters and variational calculations. The numerical diagonalization cannot deal with phenomena involving many degrees of freedom while the variational calculation is hard to control its accuracy.

We have been trying to develop general framework for overcoming this difficulty based on tensor network states. In SY2017, we studied $S = 1$ bilinear-biquadratic model on the star lattice, which is the kagome lattice with each lattice point replaced by a bond. The Hamiltonian is defined as

$$H = \sum_{(ij)} \left[\cos \phi \, (S_i \cdot S_j) + \sin \phi \, (S_i \cdot S_j)^2 \right]$$

Similar to the kagome lattice, antiferromagnets on this lattice have a strong quantum fluctuations that may lead to spin liquid states.

We carried out the iPEPS calculation using the original code based on mptensor [2]. Since the final state depends on the initial condition and the restriction we impose, we tried various sets of the initial conditions and the ansatz for each value of ϕ and chose the state with the lowest energy. We discovered four phases: (1) the ferromagnetic phase ($0.5\pi < \phi < 1.25\pi$), (2) the ferroquadrupolar phase ($1.25\pi < \phi < 1.75\pi$), (3) the antiferromagnetic phase ($1.75\pi < \phi < 0.02\pi$), and (4) the spin liquid phase ($0.02\pi < \phi < 0.5\pi$) In particular, for the spin liquid phase, we found

that the method of symmetric simple update, which enforces the symmetry, yielded the best results among all the trials. While this itself is a strong evidence for the liquid nature of this phase, we confirmed the result by computing the correlation length (Fig.1 (c)). The estimation of the correlation length was performed through the computation of the eigenvalues of the transfer matrix constructed from the edge tensor. (ϵ_i ($i = 0, 1, 2, 3$) in Fig.1(b)) It is clear that the correlation length saturates with finite value as the bond dimension increases.
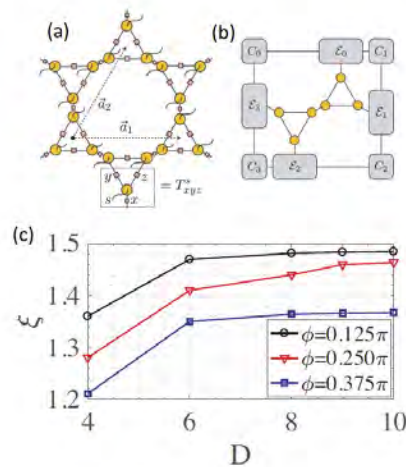

Figure 1: (a) The star lattice. (b) The corner transfer matrix configuration. (c) The correlation length as a function of the bond dimension.

[1] This report is based on Hyun-Yong Lee and Naoki Kawashima arXiv:1802.10281.

[2] https://github.com/smorita/mptensor

Simulation of organic-inorganic interfaces

Shuji OGATA

Nagoya Institute of Technology

Gokiso-cho, Showa-ku, Nagoya 466-8555, Japan

In the fiscal year of 2017, we have addressed three subjects using our order-N DFT code (DC-RGFT) and hybrid quantum-classical (QM-CL) simulation code.

Subject 1: Chemical Reactions Involved in Moisture-Induced Weakening of Adhesion Between Aluminum and Epoxy Resin. The adhesive bonding of metals using epoxy resin is an important technology in manufacturing industries. It is well known that adhesion strength becomes significantly reduced in a moist environment. To understand the mechanisms at the electronic structure level, we perform hybrid QM-CL simulations on various Al and epoxy resin interface systems with water molecules inserted in the contact region. In accordance with experimental conditions, the Al layer is surface oxidized to a depth of 10 Å while the bisphenol-A type epoxy molecule has both OH and ether groups. Shear deformations are simulated using the hybrid quantum-classical method in which about 1,500 atoms at the contact region are treated with density functional theory. For the first time, calculated adhesion strengths compare well with the experimental values. Three types of chemical reactions that affect the adhesion strength occur depending on the terminal functional groups of the Al oxide surface and the water layer formation. Separate calculations confirm small barrier energies for all the reaction processes.

Subject 2: Efficient Calculation Scheme for the Work of Adhesion between a Liquid and Polymer-Grafted Substrates [1]. Complex solid surfaces, such as polymer-grafted surfaces, are used in industrial applications; however, nearly all existing methods are applied to a flat solid surface. We therefore use molecular simulation to develop a novel method for the calculation of the work of adhesion between a liquid and a solid surface. Herein, we separate liquid molecules from the solid surface based on their shape by placing spherically symmetric potentials around atoms selected from the substrate and graft polymers onto them. To avoid the deterioration of accuracy numerical integrations, we update parameters that appear in the potential to suppress sharp variations in the gradient of free energy. This method is applied to the interface between water and gold substrate modified by poly(ethylene oxide) (PEO), revealing that the work of adhesion is greater at intermediate PEO densities.

Subject 3: Large-Scale DFT Simulation of Li-atom Insertion and Extraction in Quinons@SWCNT Rechargeable Battery Cathodes [2]. The system of quinone molecules encapsulated in the single-wall carbon nanotube (SWCNT) has been proposed as a next-generation cathode electrode material for rechargeable battery. We investigate the complex interaction among the SWCNT, phenanthrene-quinone (PhQ), and Li atoms in the encapsulated system by using DC-RGDFT. We thereby find that the shape of the SWCNT changes significantly in the relaxed state depending on the extent of Li atoms inserted. In a typical run using 63 CPU's, it takes about 9 minutes to evolve the atomic dynamics by a timestep; here, the settings of the parallel computation are the - spatial decomposition of 5x5x5, the electronic level parallelization of 2, and the OpenMP parallelization of 4.

References

[1] M. Urangase and S. Ogata, MRS Adv. **3** (2018) 519-524.
[2] M. Tsuzuki, S. Ogata, and M. Uranagase, MRS Adv. (2018) 1-6, in press.

Analyses of momentum-dependent excitations in hole-doped cuprates observed by inelastic x-ray scattering at the oxygen K edge

Takami TOHYAMA

Department of Applied Physics, Tokyo University of Science, Tokyo 125-8585

Resonant inelastic x-ray scattering (RIXS) is a powerful tool to identify spin and charge excitations in strongly correlated electron systems. RIXS at oxygen K edge in hole-doped cuprates can detect both charge and two-magnon excitations. Recent O K-edge RIXS for $La_{2-x}(Br,Sr)_x CuO_4$ has observed clear momentum $\mathbf{q}$ dependence below 1 eV [1]. The broad spectral weight exhibits positive dispersion and shifts to higher energy with increasing x. In order to clarify the origin of the dispersion, it is necessary to compare the experimental data with theoretical calculations.

In this project, we calculated the dynamical charge structure factor on oxygen orbitals in a three-band Hubbard model by the dynamical density-matrix renormalization group (mainly using the K-computer) and found that the calculated result is consistent with the experiments [1]. Therefore, the $\mathbf{q}$ dependent spectral weight can be ascribed to charge excitations. However, before concluding this, we have to deny a possibility of two-magnon excitations.

We calculate the $\mathbf{q}$ dependent two-magnon excitations for the t-t'-t''-J model with three-site terms, which is one of a realistic models for cuprates, and compare them with charge excitations as shown in Fig. 1. We find that the $\mathbf{q}$ dependence mainly appears for the low-energy region less than energy $\omega = t \sim 0.35$ eV. This energy region is smaller than the region where the RIXS data shows a dispersive mode. In contrast, the $\mathbf{q}$ dependent charge excitations appears even for the high-energy region up to
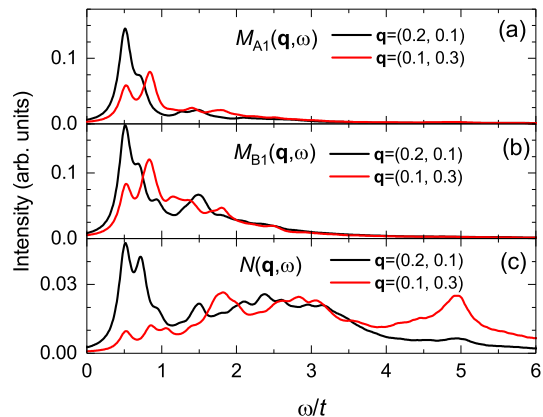

Figure 1: Dynamical two-magnon correlation function for (a) A_1 mode, (b) B_1 mode, and (c) dynamical charge structure factor at $\mathbf{q}/\pi = (0.4, 0.1)$ (black line) and $(0.1, 0.3)$ (red line) for a 2-hole $\sqrt{20} \times \sqrt{20}$ periodic lattice of the t-t'-t''-J model with three-site terms: $t = 1$, $t' = -0.25$, $t'' = 0.12$, and $J = 0.4$.

$\omega = 6t \sim 2$ eV. This suggests that two-magnon excitations are not the origin of the observed $\mathbf{q}$ dependent excitations.

We therefore conclude that the $\mathbf{q}$ dependent spectral weight observed by O K-edge RIXS is ascribed to intraband charge excitations that exhibit damped and incoherent characters inherent in doped Mott insulators.

References

[1] K. Ishii, T. Tohyama *et al.*: Phys. Rev. B **96** (2017) 115148.

Conversion and storage of energy−fuel cells and secondary batteries: Research and development of fundamental technologies of battery simulators.

Susumu OKAZAKI

Department of Materials Chmistry, Nagoya University

Furo-cho, Chikusa-ku, Nagoya 464-8603

The goal of our project is to develop the basic technology of the whole battery simulator. One of the key techniques is molecular-level design of polymer membranes controlling transportation of protons and ions across the membrane with proper stiffness resistant to mechanical deformation under external stress. Such membranes are widely applicable to the fuel cells used in the industrial products.

On the system B, we performed fully atomistic molecular dynamics (MD) calculations of hydrated perfluorosulfonic acid (PFSA) ionomers composed of a hydrophobic polytetrafluoroethylene backbone with hydrophilic side chains terminated by sulfonic acid[1], as a model of proton exchange polymer electrolyte membrane of fuel cells (Figs. 1 and 2). On the basis of these atomistic MD calculations, we constructed a predictive coarse-grained (CG) model for the structure and morphology of PFSA membranes[2]. The CG model reproduced reasonably both the thermodynamic and structural properties of the PFSA membrane for all examined water contents, and has considerable potential for application to realistic long-chained PFSA membranes. Furthermore, in order to realize a tensile test of polymer materials by a large scale MD calculation, we derived microscopic expression of the pressure tensor using the fast multipole method (FMM) with periodic boundary conditions[3]. These results will contribute to the development of higher performance fuel−cells and sec-
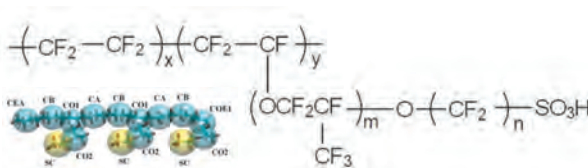

Figure 1: Molecular structure of perfluorosulfonic acid (PFSA) ionomers. Inserted figure is the CG model of PFSA ionomers[2].
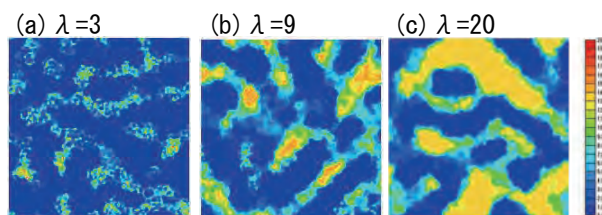

Figure 2: Number density map of sulfonic acid groups, water, and hydronium ions at one cut plane. λ is a mole fraction of water molecule and hydronium ion to sulfonic acid groups.

ondary batteries and to the realization of the entire battery simulator in the near future.

References

[1] A. T. Kuo, W. Shinoda, S. Okazaki : J. Phys. Chem. C **120** (2016) 25832.

[2] A. T. Kuo, S. Okazaki, W. Shinoda : J. Chem. Phys. **147** (2017) 094904.

[3] N. Yoshii, Y. Andoh, S. Okazaki, J. Comput. Chem., in press.

Excited-state calculations for molecular aggregates based on Green's function and fragmentation methods

Takatoshi Fujita

Institute for Molecular Science
Myodaiji, Okazaki, Aichi 444-8585

Predicting the energies of charged and neutral excitations is essential for understanding charge transport and optical properties of organic materials. However, quantitative calculations of the electronic states are still difficult due to the interplay of electronic polarization and charge delocalization effects. It is established by photoelectron spectroscopy studies that the ionization potential (IP) and electron affinity (EA) of isolated molecule are significantly different from those of solid phase. One factor contributing the difference is the polarization effects, which originates from the screening of the charge by the electronic polarization of the surrounding molecules. Another factor is the band dispersion; the orbital interactions between highest-occupied molecular orbitals (HOMOs) and lowest-unoccupied molecular orbitals (LUMOs) result in the valence- and conduction-band dispersion, respectively. Therefore, describing the charge delocalization and electronic polarization effects is of critical importance for accurate predictions of the energy levels of quasiparticles.

We have been developing the fragment-based method for calculating charge transport mobilities [1] and electronically excited states. [2] Our method relies on the fragmentation approach; the total system is first divided into a lot of small parts called fragments, and the diabatic statics are defined by the electronic structure calculations of fragment monomers embedded in the electrostatic potential from other fragments. The delocalization effects can be restored by calculating Hamiltonian matrix elements among diabatic states. We have recently shown that the fragment-based approach can provide reasonable and efficient description of electronically excited states of molecular aggregates. [2] The ground-state electronic polarization can be accurately treated by the self-consistent determination of charge density. However, our scheme is incapable to treat induced polarizations after electronic excitations. In this study, we incorporate many-body Green's function theory into the FMO method so that both charge delocalization and electronic polarization can be treated on the same footing.

Here, we employ GW theory [3] to describe electronic polarization effects. Within the GW, the dielectric function is computed for screened Coulomb interactions, and the self-energy is expanded with respect to the screened Coulomb interaction. Following the standard notation, the self-energy and screened Coulomb interaction are calculated according to

$$\Sigma(r, r', \omega) = \tag{1}$$
$$\frac{i}{2\pi} \int d\omega' G(r, r', \omega + \omega') W(r, r', \omega) e^{i\omega\eta},$$

$$G(r, r', \omega) = \sum_p \left[\frac{\psi_p(r)\psi_p^*(r')}{\omega - \epsilon_p + i\eta sgn(\epsilon_p - E_F)} \right], \tag{2}$$

$$W(r, r', \omega) = v(r, r) + \tag{3}$$
$$\int dr_1 dr_1 v(r, r_1) \chi_0(r_1, r_2, \omega) W(r_2, r', \omega).$$

We have developed the fragment-based scheme to calculate the quantities above. The one-body Green's function is approximated as a sum of Green's functions of fragment monomers and dimer corrections. On the other hand, we approximated the independent-electron susceptibility from those of fragment monomers, $\chi^0 = \sum_I \chi_I^0$, and defined the screened-Coulomb potential of the total system. Our GW implementation relies on the real-space auxiliary functions. [4] The auxiliary functions are defined by the direct products of two atomic orbitals and are constructed by the Cholesky decomposition. The fragment-based GW method was incorporated into the developer version of ABINIT-MP program. [5]

As a numerical example, the crystal structure of pentacene thin film phase [6] is considered We calculate self-energy within the static Coulomb-hole plus screened exchange (COH-SEX) approximation. One-shot GW calculation was performed with 6-31G* basis set and B3LYP reference. Quasiparticle energies of a pentacene monomer are -6.97 (HOMO) and -1.29 eV (LUMO). The FMO-GW calculation was performed for the thin film structure containing 39 pentacene molecules (Fig.1). The quasiparticle energies were calculated in the range from -6.77 to -6.15 eV for HOMOs and from -1.92 to -1.29 eV for LUMOs. Diagonalization of the HOMOs and LUMOs with transfer integral yields the band gap as 4.03 eV. This significant reduction of the band gap dominantly arises from the electronic polarization effects.
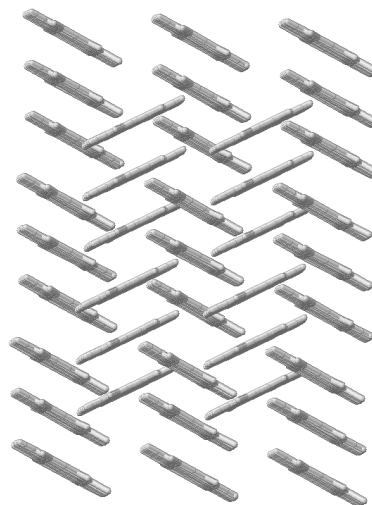

Figure 1: Crystal structure of pentacene thin film.

References

[1] T. Fujita, Y. Haketa, H. Maeda, Y. Mochizuki, Org. Electron. **49** (2017) 53.

[2] T. Fujita, Y. Mochizuki, J. Phys. Chem. A **11** (2018) 3886.

[3] L. Hedin, Phys. Rev. **139** (1965) A796.

[4] X. Ren, P. Rinke, V. Blum, J. Wieferink, A. Tkatchenko, A. Sanfilippo, K. Reuter, M. Scheffler, New. J. Phys. **14** (2012) 053020.

[5] S. Tanaka. Y. Mochizuki, Y. Komeiji, Y. Okiyama, K. Fukuzawa, Phys. Chem. Chem. Phys. **16** (2014) 10310.

[6] S. Schefer, M. Huth, A. Dobrinevski, B. Nickel, J. Am. Chem. Soc. **129** (2007) 10316.

Materials design for energy-saving and energy-creation materials

Tetsuya FUKUSHIMA

Institute for NanoScience Design, Osaka University, Osaka 560-8531, Japan
Institute for Datability Science, Osaka University, Osaka 565-0871, Japan

A "scale-bridging" simulation technique, combining the Korringa-Kohn-Rostoker (KKR) Green's function method and model approaches, was developed this year. On the basis of the "scale-bridging" simulation technique and massively parallel computing, we designed new energy-saving and energy-creation materials, such as high entropy alloys [1], thermo electric materials [2], and dilute magnetic semiconductors (DMSs) [3]. Here, we introduce the materials design of Ge type DMS systems.

Recently, the IV-type semiconductor Ge has attracted much attention as the host material of ferromagnetic DMSs for the following two reasons: (i) Ge possesses higher mobility than that of Si; therefore, it has the possibility of the realization of high-speed and low-power consumption LSI systems; (ii) Ge has a good compatibility with the Si-CMOS technology. We performed the density functional theory calculations or transition-metal (TM) impurities doped Ge by using the KKR Green's function method with the coherent potential approximation (CPA), to theoretically shed light on the ferromagnetic mechanisms of the Ge-based DMS systems.

Our calculations indicated that the ferromagnetic interactions by the double exchange mechanism are dominant for the Fe- and Co-doped Ge systems. However, these ferromagnetic interactions are quite short ranged compared to the (Ga,Mn)As, and are also weak compared to (Ga,Mn)N, so that we cannot expect high ferromagnetic Curie temperature (T_C) in terms of the magnetic percolation effect if the TM impurities are homogeneously distributed in the hosts. Antiferromagnetic states are stable for the V-, Cr-, and Mn-doped Ge, and the Ni-doped system becomes a nonmagnetic. The inhomogeneity of the TM impurities drastically changes the magnetic states and has a crucial role in the experimentally observed high-T_C ferromagnetism in the IV-type DMSs. The cluster expansion method revealed that the Mn-doped Ge systems tend to generate ordered compounds, such as Ge_3Mn_5 and Ge_8Mn_{11}, at Mn-rich regions. These precipitated ordered compounds are the causes of the ferromagnetism in (Ge,Mn); in particular T_C of Ge_3Mn_5 is consistent with the experimentally observed T_C of (Ge,Mn).

The electronic structure of (Ge,Fe) calculated by the variational pseudo-self-interaction-corrected method reproduces the spectra of the Fe-3d states in the SX-ARPES experiment. It was proven by the multi-scale (scale-bridging) simulations that the Fe atoms are not randomly distributed in the Ge host but gathered with keeping the diamond structure by the attractive pair interactions i.e., the spinodal nanodecomposition. T_C of (Ge,Fe) is enhanced by the annealing process, because the number of the first-nearest-neighbor Fe-Fe pairs with the strong ferromagnetic interaction increases by proceeding the spinodal nanodecomposition. Our simulations reproduce the experimental magnetic situation very well,

and the T_C values estimated by the random phase approximation method are in good agreement with the observed values.

We emphasize that the manipulation of structural, configurational, and spin disorders in DMS systems are very important to obtain colossal magnetic responses. In particular, there is the possibility that a drastic magnetic transition between ferromagnetism and antiferromagnetism can be realized in the Ge-doped DMSs by controlling the nanostructure and dimensionality, and applying the gate voltage. Additionally, compared to the typical III-V and II-VI DMSs, the Ge-based DMSs are rather compatible with the present CMOS technology. Utilizing the Ge-based DMSs is a good way to realize next-generation devices based on semiconductor spintronics.

References

[1] T. Fukushima, H. Katayama-Yoshida, K. Sato, M. Ogura, R. Zeller, and P. H. Dederichs: J. Phys. Soc. Jpn. **86** (2017) 114704.

[2] H. Shinya, A. Masago, T. Fukushima, and H. Katayama-Yoshida: Jpn. J. Appl. Phys. **56** (2017) 081201.

[3] H. Shinya, T. Fukushima, A. Masago, K. Sato, and H. Katayama-Yoshida: Phys. Rev. B **96** (2017) 104415.

Exploration of novel oxide and nitride semiconductors using first-principles calculations

Fumiyasu OBA[1,2] and Yu KUMAGAI[2]

[1]*Laboratory for Materials and Structures, Institute of Innovative Research,*
Tokyo Institute of Technology,
4259 Nagatsuta, Midori-ku, Yokohama 226-8503, Japan
[2]*Materials Research Center for Element Strategy,*
Tokyo Institute of Technology,
4259 Nagatsuta, Midori-ku, Yokohama 226-8503, Japan

The search for novel semiconductors is increasingly important as the applications of semiconductors become more prevalent. Among the compound semiconductors, nitrides and oxides are especially attractive because of the abundant nitrogen and oxygen constituents. Currently commercialized nitride semiconductors are, however, mostly limited to GaN and its based alloys. Several kinds of oxide semiconductors are used in commercial applications such as transparent electrodes and thin-film transistors, but those with improved or different functionalities are required to expand the applications. This situation stimulates not only experimental but also computational exploration of novel nitride and oxide semiconductors.

It is our objective to explore novel nitride and oxide semiconductors with a wide variety of chemical compositions, crystal structures, and properties via high-throughput screening using first-principles calculations. We have been developing methods for predicting fundamental bulk and defect properties systematically [1, 2, 3, 4, 5] and applying them to the search for novel semiconductors such as ternary zinc nitrides [6]. The screening needs to be extended so that a larger number of candidate materials can be evaluated efficiently within feasible computational time whereas sufficient accuracy is kept. In this respect, an appropriate choice of the exchange-correlation functional in density functional theory is important. Therefore, the performance of several types of generalized gradient approximation (GGA) and meta-GGA functionals was systematically assessed using the allocated CPU time. We took elementary substances and binary oxides as test sets because experimental values for fundamental properties and structural parameters are available.

As examples of the results, Fig. 1 shows relative stability of polymorphs of binary divalent cation oxides obtained using the projector augmented-wave method [7] and the PBEsol functional [8] as implemented in the VASP code [9, 10]. Experimentally well-known phases are predicted to be stable among the polymorphs of each oxide. Although explicit comparison of relative formation energies between theory and experiment is difficult because of the lack of experimental values in many cases, systematic assessment on the cohesive energies of elementary substances and the formation energies of binary oxides, as well as their crystal structures, indicated improved accuracy by the PBEsol over the standard PBE functional [11].
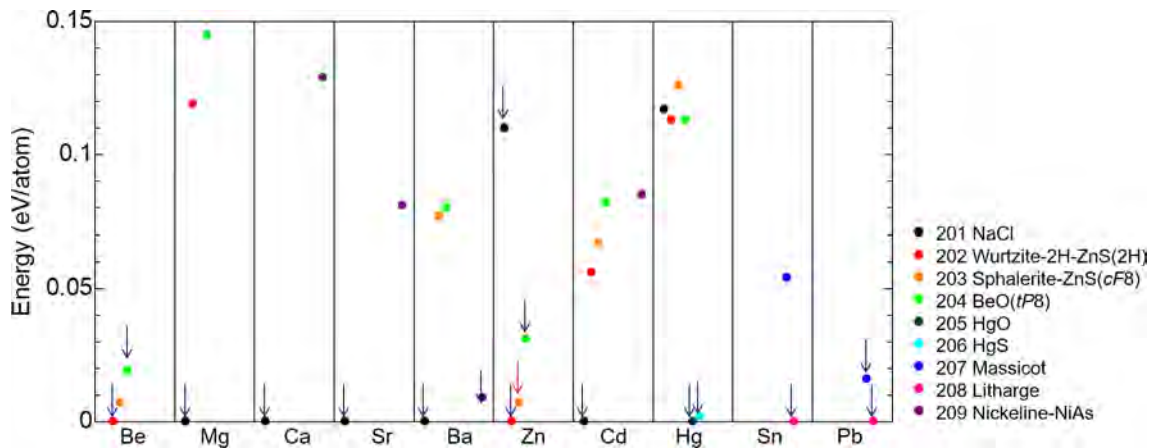
Figure 1: Relative stability of polymorphs of binary divalent cation oxides obtained using the PBEsol functional [11]. Energies are shown with respect to that of the lowest energy phase for each oxide. Experimentally reported phases are arrowed.

References

[1] Y. Kumagai and F. Oba: Phys. Rev. B **89** (2014) 195205.

[2] A. Grüneis, G. Kresse, Y. Hinuma, and F. Oba: Phys. Rev. Lett. **112** (2014) 096401.

[3] Y. Hinuma, A. Grüneis, G. Kresse, and F. Oba: Phys. Rev. B **90** (2014) 155405.

[4] Y. Hinuma, G. Pizzi, Y. Kumagai, F. Oba, and I. Tanaka: Comput. Mater. Sci. **128** (2017) 140.

[5] Y. Hinuma, Y. Kumagai, I. Tanaka, and F. Oba: Phys. Rev. B **95** (2017) 075302.

[6] Y. Hinuma, T. Hatakeyama, Y. Kumagai, L. A. Burton, H. Sato, Y. Muraba, S. Iimura, H. Hiramatsu, I. Tanaka, H. Hosono, and F. Oba: Nat. Commun. **7** (2016) 11962.

[7] P. E. Blöchl: Phys. Rev. B **50** (1994) 17953.

[8] J. P. Perdew, A. Ruzsinszky, G. I. Csonka, O. A. Vydrov, G. E. Scuseria, L. A. Constantin, X. Zhou, and K. Burke: Phys. Rev. Lett. **100** (2008) 136406.

[9] G. Kresse and J. Furthmüller: Phys. Rev. B **54** (1996) 11169.

[10] G. Kresse and D. Joubert: Phys. Rev. B **59** (1999) 1758.

[11] Y. Hinuma, H. Hayashi, Y. Kumagai, I. Tanaka, and F. Oba: Phys. Rev. B **96** (2017) 094102.

Development of Permanent Magnet Materials

Takashi MIYAKE

CD-FMat, AIST

Umezono, Tsukuba, Ibaraki 305-8568

Finite-temperature magnetism of rare-earth magnet compounds is an issue in developing high-performance permanent magnets. It is known that the intersite magnetic exchange coupling between the rare-earh and transition-metal sites, J_{RT}, plays an important role in the magnetocrystalline anisotropy at finite temperatures. We have computed J_{RT} in $NdFe_{12}$ and $NdFe_{12}X$ (X=B, C, N, O, F) based on density functional theory and Liechtenstein's method using Akai-KKR. We found that J_{RT} is sensitive to X. Especially, the Nd-Fe($8j$) coupling is significantly reduced for X=N. This suggests that the magnetocrystalline anisotropy decays quickly with increasing temperature in the X=N system, although N enhances the Curie temperature. The Nd-Fe($8j$) coupling has strong correlation with the local magnetic moment at Nd site, which is
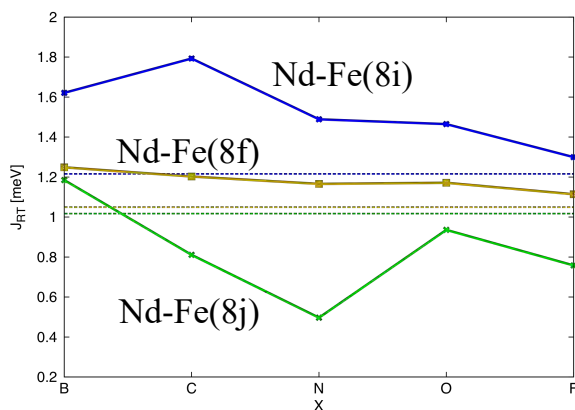
Partial substitution of Fe sites also affects finite-temperature magnetism. We have studied the Curie temperature of $NdFe_{12-x}Cr_x$ in the mean-field approximation. We found that the Curie temperature has strong dependence on the Cr concentration x. It increases with increasing x at low concentration, then turns to decrease above $x \sim 0.75$. We found that both of the following two effects are important for the increase in the small x region. The first effect is that Fe-Fe couplings are partially replaced with stronger Fe-Cr couplings by Cr substitution, which raises the Curie temperature. The other is that introduction of Cr makes surrounding Fe atoms Co-like, which enhances the Fe-Fe coupling [2].

Another important issue is crystal structure prediction of magnetic compounds. We have developed a crystal structure prediction technique in which stable structures are efficiently selected from candidate structures by Bayesian optimization. Applications to Y_2Fe_{17} and NaCl show that the number of searching trials required to find the minimum structure is reduced by 30-40% compared to random search [3].

Figure 1: Magnetic exchange coupling between the Nd and Fe sites in $NdFe_{12}X$.

References

[1] T. Fukazawa et al.: J. Appl. Phys. **122** (2017) 053901.

[2] T. Fukazawa et al.: J. Phys. Soc. Jpn. **87** (2018) 044706.

[3] T. Yamashita et al.: Phys. Rev. Materials **2** (2018) 013803.

Materials design using B, C, and N for next-generation device

Susumu SAITO

Department of Physics, Tokyo Institute of Technology

2-12-1 Oh-okayama, Meguro-ku, Tokyo 152-8551

The hexagonal BN (h-BN) atomic-layer materials are known to possess atomically flat geometries and can serve as the highest-quality substrate for other conducting and semiconducting atomic-layer materials including graphene and transition-metal dichalcogenide atomic-layer materials. We have studied the electronic properties of pristine h-BN atomic layers and their doped phases with substitutional C impurities in the framework of the density-functional theory to investigate the possibilities of utilizing h-BN materials themselves as next-generation semiconductor device materials. In this study we have used the quantum ESPRESSO package.

In our previous work [1] we have clarified that the h-BN bilayers can possess different electronic properties depending on the stacking sequence of two h-BN layers since the h-BN sheet can have two different orientations unlike graphene. We have extended this orientation dependent electronic-structure study for trilayer h-BN systems [2]. Interestingly, it is found that trilayer h-BN can have much more variations than bilayer h-BN, and that the C-doped layer and the conductive layer can become different from each other. This spatial separation of

carriers and dopants are of importance in utilizing the h-BN systems as device materials. These interesting and important properties clearly show that h-BN atomic layers are actually the potential nanoelectronics device materials in the future.

We have also studied the electronic properties of the hetero-atomic-layer systes of graphene and h-BN layer [3]. The scanning-tunneling Microscope (STM) images of these hetero atomic layers with the substitutional C impurity at the B or N site in the h-BN layer are simulated. It is found that in the case of the C dopant at the N site of the h-BN layer, its presence can be clearly detected by the STM even from the images taken atop the graphene surface layer. On the other hand, the C dopant at the B site can be detected only by the STM images taken from the h-BN surface.

In addition to the above atomic-layer materials, we have also studied the electronic properties of sp^3 carbon network materials, *i.e.* diamond, with possible polytypes. It is well-known that in the case of SiC there are various polytypes called 3C, 4H, 6H and so on. In the case of diamond, 2H has been already found in addition to the ordinary 3C diamond.

Previously we showed from the constant-temperature molecular-dynamics study that the carbon nanotube solid can transform into various sp^3 carbon phases including 2H and 4H diamond phases under moderate pressure (10 GPa to 20 GPa). From the electronic-structure study using the GW approximation and the Bethe-Salpeter analysis, we have newly clarified the polytype dependent electronic properties of diamond [4].

References

[1] Y. Fujimoto and S. Saito, Phys. Rev. B **94**, 245427 (2016).

[2] Y. Matsuura, Y. Fujimoto, and S. Saito, to be published.

[3] T. Haga, Y. Fujimoto, and S. Saito, to be published.

[4] M. Sakurai, J. R. Chelikowsky, S. G. Louie, and S. Saito, Phys. Rev. Materials **1**, 054603 (2017).

Structures and local magnetic properties of magnetic-material interfaces

Yoshihiro GOHDA

Department of Materials Science and Engineering, Tokyo Institute of Technology
J1-3, Nagatsuta-cho 4259, Midori-ku, Yokohama 226-8502, Japan

Multiferroic materials are of significant interest, because their magnetization can be controlled by the electric field, not by the electric current, which suppresses energy dissipation by the Joule heating [1]. In particular, multiferroic interfaces are good candidates for practical applications: The magnetoelectric coupling in known single-phase multiferroic materials is too weak. Even though interface multiferroicity has been studied intensively for ferromagnetic/ferroelectric interfaces [1, 2], ferromagnetic/multiferroic interfaces should be better, because the interface multiferroicity can be enhanced by the single-phase multiferroicity. First-principles calculations of ferromagnetic/multiferroic interfaces are extremely demanding due to non-collinear configurations of the magnetic moments. For example, $BiFeO_3$ (BFO) has canted magnetization by two nearly-antiparallel Fe magnetic moments due to the Dzyaloshinskii–Moriya interaction.

In this study, we demonstrate the magnetoelectric coupling for a ferromagnetic/multiferroic interface, bcc-Fe/BiFeO$_3$(001) [3]. First-principles calculations were performed on the basis of density functional theory with the generalized gradient approximation by the OpenMX code [4]. For the Fe $3d$ orbitals within BFO, the DFT+U method was used. Considering non-collinear magnetism with the spin-orbit coupling, we successfully reproduced the canted magnetization of BFO due to the Dzyaloshinskii–Moriya interaction. We examined various interfaces by changing the termination and the stacking positions at the interface. We have found that the most suitable interface for evaluating magnetoelectric coupling is the BiO-terminated interface with the bcc-Fe atoms stacked on the bridge sites of BFO(001). With the reversal of the electric polarization of BFO, a drastic change in the directions of exchange-coupled magnetization of bcc Fe and BFO has been obtained as the interface magnetoelectric effect [3]. In addition, the enhancement of the magnetic moment of interface Fe atoms in bcc Fe was found as shown in Fig. 1.
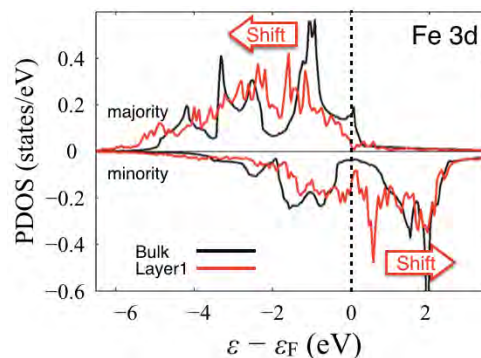

Figure 1: The calculated partial density of states of the Fe $3d$ states in bcc-Fe/BFO(001). The energy origin is set at the Fermi energy ε_F.

[1] T. Taniyama, J. Phys.: Condens. Matter **27**, 504001 (2015).

[2] C.-G. Duan, S. S. Jaswal, and E. Y. Tsymbal, Phys. Rev. Lett. **97**, 047201 (2006).

[3] K. Fujita and Y. Gohda, in preparation.

[4] T. Ozaki, Phys. Rev. B. **67**, 155108 (2003).

Magnetization Process of Permanent Magnets Revealed by Large-scale Simulation

Hiroshi Tsukahara, and Kanta Ono

High Energy Accelerator Research Organization (KEK)

1-1 Oho, Tsukuba, Ibaraki 305-0801 Japan

High-performance permanent magnets are receiving increased attention owing to shifting toward electric vehicles globally. It is indispensable to improve electric motors for power saving electric vehicles, and the permanent magnet is one of the most important parts of the electric motor. The performance of the permanent magnet is governed by coercivity and remanent magnetization. When applied magnetic eld approaches the coercivity, nucleation cores are created, and domain walls move inside the permanent magnet. Because magnetization reversal regions are expanded by the motion of the domain wall, it is important for improvement of the permanent magnet to clarify details of the domain wall motion.

Micromagnetic simulations have revealed the magnetization dynamics within magnetic materials including the permanent magnet. The micromagnetic simulation enables us to observe the motion of the domain wall numerically. However, average diameters of grains which consist of the permanent magnet exceed 1.0 μm, and a length of the domain wall is approximately 5 nm. Hence, massively parallel computing is essential to investigate the magnetization dynamics inside the permanent magnet. [1]

We implemented 3 dimensional fast Fourier transform (FFT) subroutine based on MPI parallelization using GPGPU computing and calculated magnetic dipolar elds which occupy over 80 % of a calculation time of our CPU based simulation code. We performed
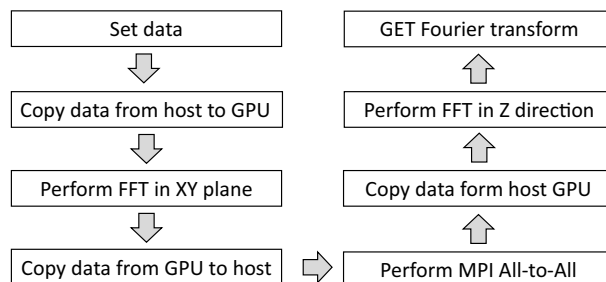

Figure 1: Algorithm of 3 dimensional FFT using GPGPU based on MPI parallelization.

fast Fourier transform using GPGPU according to the following procedure as shown Fig. 1 First, we set magnetization data which is divided into MPI processes. After copying data to GPU, we performed 2 dimensional FFT using cuFFTExecZ2Z and copied data to host. Next, we exchanged data among the MIP processes to performed FFT, and we copied data to GPU. After performing 1 dimensional FFT in the Z direction, we get the 3 dimensional Fourier transform of the magnetization.

In the case of large-scale micromagnetic simulation, a required memory capacity exceeds a memory of GPU. Hence, this study is the rst step for massively parallel computing with many GPUs.

References

[1] H. Tsukahara, K. Iwano, C. Mitsumata, T. Ishikawa, and K. Ono, Comp. Phys. C **207** (2016) 217.

Molecular simulation of ion transport and desolvation at electrode interface

Akihiro MORITA

Department of Chemistry, Graduate School of Science

Tohoku University, Aoba-ku, Sendai, Miyagi 980-8578

The present group has been studying liquid interfaces in close collaboration with interface sensitive nonlinear spectroscopy, such as sum frequency generation (SFG). In particular, this project investigates liquid-solid interfaces in relation to electrochemistry. In applying SFG to such solid-liquid interfaces, however, the spectra could involve significant $\chi^{(3)}$ effect, which influences on the interpretation of the spectra. The excess charge at solid surface may generate a static electric field which penetrates into the liquid and induce additional source of SFG signal. Consequently, the observed SFG signal contains substantial contribution from the region affected by the static field ($\chi^{(3)}$ contribution). In recent applications to solid-liquid interfaces, reliable estimate of c(3) contribution has been an critical concern.

It is not straightforward to separate the intrinsic surface signal of $\chi^{(2)}$ and the $\chi^{(3)}$ contribution experimentally, whereas MD calculation allows for calculating the c(3) signal in a direct manner and well separating the two contributions. Therefore, we performed the computation of the $\chi^{(3)}$ signal of water for the first time, and revealed its spectral lineshape and amplitude. We also demonstrated it possible to evaluate the $\chi^{(3)}$ contribution in the observed SFG signal and to calibrate its contribution to extract the intrinsic signal from the interface.
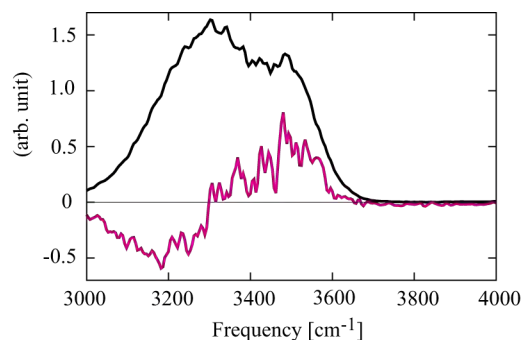

Fig. 1: Calculated Im[χ] spectrum of water-silica interface. Black line stands for the observed SFG signal, while the purple is the intrinsic $\chi^{(2)}$ signal by removing the $\chi^{(3)}$ contribution.

References

[1] T. Joutsuka, T. Hirano, M. Sprik, and A. Morita, Phys. Chem. Chem. Phys., **20** (2018), 3040-3053.